ASEG-PESA 2015
Geophysics and Geology together for Discovery
24th International Geophysical Conference and Exhibition
15–18 February 2015 Perth, Western Australia

Interpretation of 3D high–resolution seismic data collected over an IOCG deposit in South Australia

Muhammad Shahadat Hossain
PhD Student
Dept. of Exploration Geophysics
Curtin University, Perth, WA
&
Deep Exploration Technologies CRC
PO Box 66, Export Park, Adelaide Airport
South Australia 5950, Australia
Muhammad.Hossain@student.curtin.edu.au

Milovan Urosevic
Associate Professor
Dept. of Exploration Geophysics
Curtin University, Perth, WA
&
Deep Exploration Technologies CRC
PO Box 66, Export Park, Adelaide Airport
South Australia 5950, Australia
Milovan.Urosevic@curtin.edu.au

Anton Kepic
Associate Professor
Dept. of Exploration Geophysics
Curtin University, Perth, WA
&
Deep Exploration Technologies CRC
PO Box 66, Export Park, Adelaide Airport
South Australia 5950, Australia
Anton.Kepic@curtin.edu.au

SUMMARY

A 3D high–resolution seismic dataset was acquired to investigate typically complex IOCG deposits in Hillside, South Australia. Petrophysical data measured from the core samples and the density data supplied by the mining company were utilised during the volumetric interpretation. However, petrophysical data show that the boundaries between gabbro and metasediments may not generate acoustic impedance contrast to be clearly detected by seismic reflection method. The base of the top cover is mappable throughout the cube and the tops of the major formations have agreement with magnetic data. The faults extracted from the seismic volume using ant–tracking attribute have good agreement with the company supplied geological interpretation based on the drilling information.

Key words: Seismic interpretation, 3D seismic reflection, ant–tracking, hard rock seismic.

INTRODUCTION

Open–cut mining has been the most economical form of mining in Australia for the last few decades. The mining industry generally use drilling, gravity and magnetic methods, and geological mapping to explore new deposits. However, declining reserves of most mineral deposits and scarcity of new discoveries of large, near–surface deposits is forcing mineral industries to explore deeper in order to meet the future needs (Figure 1; Salisbury and Snyder, 2007). As a results, the seismic reflection method has the potency to become an important tool to delineate deep–seated structures hosting ore bodies (Malehmir *et al.*, 2012).

Gravity and magnetic methods are unable to resolve targets beyond 500 metres. High–resolution seismic reflection method renders the subsurface geologic structures at depths more than one kilometres (Salisbury and Snyder, 2007, Malehmir *et al.*, 2012). In some special cases, seismic reflection method can delineate structures up to 3 km deep; the current maximum depth of mining (Salisbury and Snyder, 2007, Malehmir *et al.*, 2012).

A comprehensive review of mineral exploration employing seismic reflection method was provided by Reed (1993). Afterwards, a number of papers were published exhibiting successful application of reflection seismic method in hard rock environment (Eaton *et al.*, 2003). Noponen *et al.* (1979) studied the reflections from discontinuities within crystalline rocks for drilling and mine–workings and concluded that the impedance contrast of most mafic rocks and high–density ores against felsic rocks are sufficient enough to generate noticeable reflections (Urosevic *et al.*, 2005, 2007).

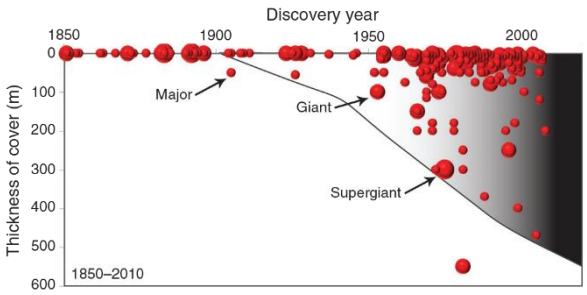

Figure 1. Depth of major mineral discoveries (bulk minerals such as coal, bauxite, and iron ore are excluded) in Australia during 1850–2010 shows a trend toward depth (Malehmir *et al.*, 2012).

The Hillside copper–gold deposit is located on the east coast of Yorke Peninsula, about 15 km south of Ardrossan, ~70 km northwest of Adelaide, South Australia. The Hillside deposit is hosted within Paleo–to–Mesoproterozoic rocks of the Olympic IOCG province that extends along the eastern margin of the Gawler Craton (Goleby et al. 2005). The evolution of the Hillside deposit started with ductile folding as a result of East–West compression and intrusion of gabbro and granite dykes took place c.1570Ma–1585Ma (Marjoribanks, 2013). Fluid flows through the tensional fractures selectively replaced favourable beds with silica, potassium–feldspar, albite, hematite, magnetite and sulphide skarns (Marjoribanks, 2013). This alteration has led to the formation of an aquitard where mineral deposition sealed the fractures. Rising fluids accumulated below the aquitard and became overpressured, eventually leading to rupture and brecciation of the seal

(Marjoribanks, 2013). Rupture created sudden pressure drops which preceded deposition of massive sulphide & magnetite as matrix to brecciated rock (Marjoribanks, 2013). Cycling of repeated sealing–brecciation–sealing process might have repeated many times along major fluid pathways leading to the production of the major ore shoots (Marjoribanks, 2013).

METHODOLOGY

In seismic interpretation, conventional interpretation methods produce maps whereas volume visualisation methods produce 3D perspectives (Kidd, 1999). In seismic volumetric interpretation the interpreter directly evaluates the seismic reflectivity of the subsurface media in three–dimensional space by applying various levels of transparency/opacity filters to the data (Kidd, 1999). This enables a range of attribute values to be modified or switched off, giving the interpreter the ability to see through the entire volume (De Pledge, 2000).

The interpretation based on 2D imaging is significantly different from the interpretation based on 3D imaging. The traditional approach is to slice the volume in the x–z or y–z planes to create inline and cross–line sections (Yilmaz, 1987). Time slices are created by slicing the volume into horizontal sections. The individual slices can be interpreted using 2D techniques but clearly valuable information gets lost when this is done since the data coherency along the axis normal to the slice plane cannot be seen (Wolfe and Liu, 1988).

In November–December 2012, Curtin University conducted a 3D high–resolution seismic acquisition survey at Rex Minerals' Copper–Gold mining project at Hillside. The seismic cube covers 0.44 km^2 area (1375m×320m). In 2013, trips to the core repository at Hillside were organised to measure petrophysical properties (e.g. P and S wave velocities, density, magnetic susceptibility) of the drilled core samples. In addition, a specific gravity voxet equal to the seismic cube was extracted from the Rex supplied density pointsets database to be used in interpretation.

PETROPHYSICAL DATA ANALYSIS

A couple of trips to the core repository at Hillside mine site were organised on 29 July–2 August 2013 and 4 November–8 November 2013 to measure petrophysical properties (e.g. P– and S–wave velocities, density, magnetic susceptibility) of the core samples.

505 samples were analysed and 471 produces P– and S–wave velocity data. The scatter plots show the petrophysical properties of different rock types (Figure 2).

The density values in Gabbro samples range from 2600 kg/m^3 to 3870 kg/m^3 with an average of 2910 kg/m^3. Granite samples range from 2610 kg/m^3 to 3840 kg/m^3 with a mean value of 2720 kg/m^3. Metasediment samples vary from 2600 kg/m^3 to 3200 kg/m^3 with a mean value of 2780 kg/m^3 and in the mineralised host rock range from 2630 kg/m^3 to 4810 kg/m^3 with an average density of 3020 kg/m^3.

Nafe and Drake (1957) used laboratory measurements and borehole data to determine the relationship between depth and porosity for shallow and deep marine sediments. They also used a simple density–porosity relationship to derive a depth–density relationship. Combining these results they were able to present a velocity–density relationship (Wyss *et al.*, 1993). During the 1960s, more data have been combined and a refined velocity–density relationship has been worked out (Ludwig *et al.*, 1970). Later, Barton (2007) applied the Nafe–Drake relationship to convert the velocity distribution of seismic models into corresponding density model. Salisbury, *et al.* (1996) measured samples of pure pyrite, chalcopyrite, sphalerite, and pyrrhotite at 200 MPa pressure to establish theoretical limits of the velocity–density field for common ores.

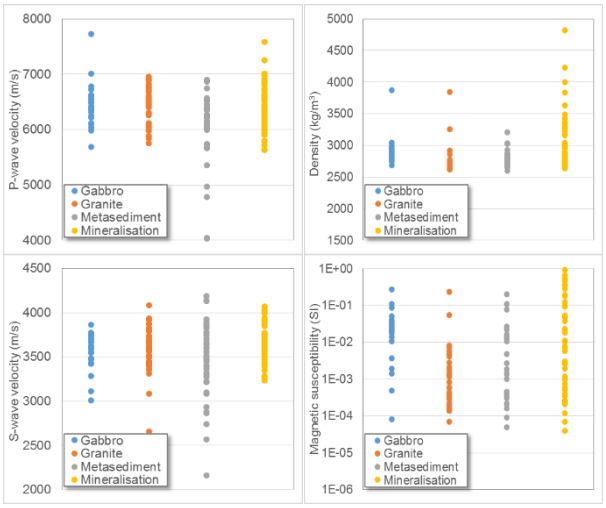

Figure 2. Petrophysical data represents P– and S–wave velocity, density, and magnetic susceptibility of the measured core samples.

Petrophysical data measured from the core samples from Hillside were plotted on the velocity–density field in order to make an assumption about the mineral composition of the rock types. Figure 3 shows the distribution of the samples on the velocity–density field.

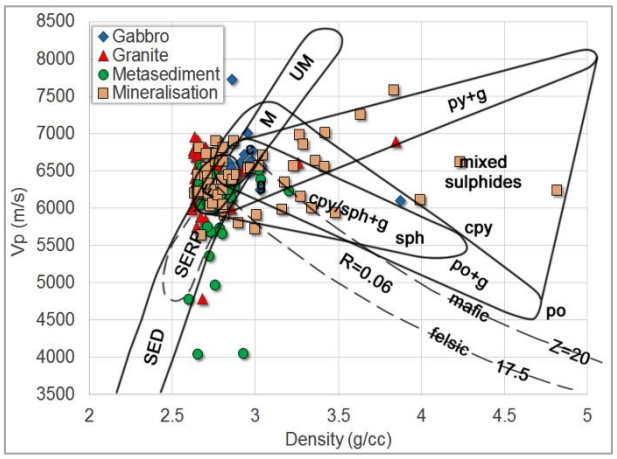

Figure 3. P–wave velocity (vp)–density fields for sulphide ores and silicate host rocks adopted from Salisbury, *et al.* (1996) were used to categorise samples from Hillside. Ores: py=pyrite, cpy=chalcopyrite, sph=sphalerite, po=pyrrhotite. Silicate rocks along Nafe–Drake curve: SED=sediments, SERP=serpentinite, F=felsic, M=mafic, UM =ultramafic, g=gangue, c=carbonate. Dashed lines represent lines of constant acoustic impedance (Z) for felsic and mafic rocks.

Most of the gabbro samples are clustered within the density–velocity field for carbonate and mafic rocks. Gabbro shows a gradual increase in P–wave velocity with increasing density whereas granite and metasediments are clustered and the P–wave velocity varies greatly even though the density does not change much. The mineralised host rock samples are scattered all over the velocity–density fields suggesting that the samples differ greatly in mineral composition.

SEISMIC VOLUMETRIC INTERPRETATION

Seismic Attributes are all the information obtained from seismic data, either by direct measurements or by logical or experience based reasoning (Taner, 2001). A number of attributes were computed to help the edge detection and enhancement process in order to identify faults.

The only horizon was extracted using 70% seed confidence and the interpolation was validated over an expansion of 3×3 volume (Figure 4). Densely populated seed points were used to maintain a high surface stability index.

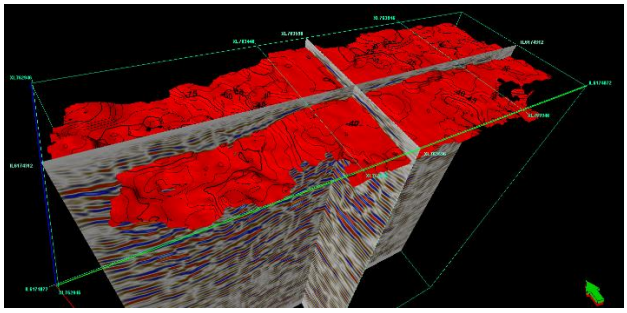

Figure 4. Horizon extracted using densely populated seed points. 2D, 3D, guided, and manual seeding methods were used to maintain high surface stability index during the horizon extraction process.

Fault attributes were extracted using GoScope plugin in Paradigm GOCAD 2011.2 using a correlation window length of 20 and sliding window length of 10. Suitable pointsets were then joined together to form manually interpreted fault surfaces. Automatic fault extraction was done on the seismic volume using patent–pending ant–tracking method. The ant–tracking method is a coherent signal tracker based on “swarm intelligence” to find optimal connectivity for fault features within an edge detected volume. The first step in the ant–tracking algorithm, each agent makes an estimate of the orientation for the identified local maximum within the agent's territory. This orientation estimate defines the tracking direction for that agent. The agents are restricted to a maximum of 15% deviation from this original orientation estimate. Also, the movement of the ant agents is performed in steps (Ant step size), a step is defined in voxels (Schlumberger, 2013).

The ant–tracking process can be divided into four main activities: i) seismic conditioning, ii) edge detection, iii) edge enhancement, and iv) surface extraction.

Seismic conditioning is performed by running a number of filter attributes (bandpass filter, median filter, structural smoothing etc., Figure 5).

The second step enhances the spatial discontinuities in the seismic volume using coherency/similarity attributes e.g. variance, chaos, dip deviations etc. (Figure 6). The third step generates the ant–tracked volume, which significantly improves the fault attributes by suppressing noise and remains of non–faulting events (Schlumberger, 2013).

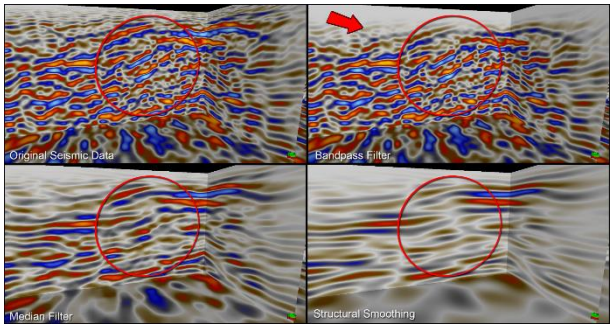

Figure 5. Seismic condition performed on the original seismic volume by applying various filters e.g. bandpass filter, median filter, structural smoothing etc.

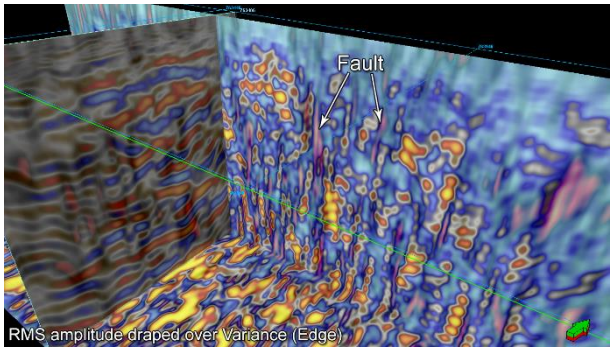

Figure 6. Variance attribute (edge method) draped over RMS amplitude shows enhanced spatial discontinuities in the seismic volume (Hossain *et al.*, 2014).

The process is achieved emulating ant colony behaviour in nature and how they use pheromones to mark their paths in order to optimize the search for food. Using the same approach, "artificial ants" are used as seeds on a seismic volume to look for fault zones. The result is an attribute volume with very sharp and detailed fault zones (Schlumberger, 2013; Figure 7).

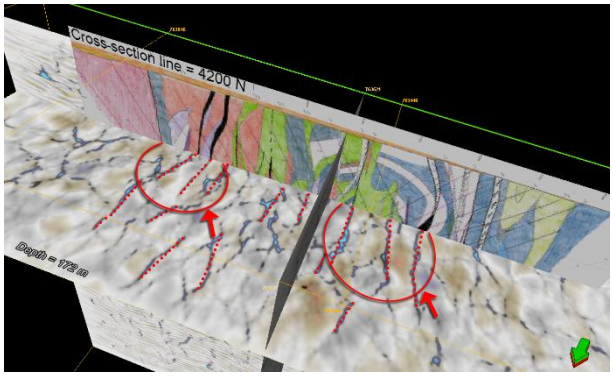

Figure 7. Faults extracted using ant–tracking method on Hillside 3D seismic volume. A geological cross–section was used to show the coherency of the extracted faults with geological interpretation (Hossain *et al.*, 2014).

CONCLUSIONS

Density values measured from the core samples and the supplied density database show that the average density of gabbro, granite, and metasediments are different from each other. However, the density of gabbro overlaps with the density of metasediments between 2.7 and 3 suggesting that the density contrast at the boundaries between gabbro and metasediments may not be sufficient enough to generate acoustic impedance contrast to be detected by the seismic reflection method. Faults extracted using the ant–tracking method have good agreement with the company supplied geological interpretation based on the drilling information.

ACKNOWLEDGEMENTS

This work has been supported by the Deep Exploration Technologies Cooperative Research Centre whose activities are funded by the Australian Government's Cooperative Research Centre Programme. This is DET CRC Document 2014/544. I would also like to thank Rex Minerals Copper–Gold Mining Project at Hillside, South Australia for providing an outstanding support.

REFERENCES

De Pledge, J.E., 2000, Derivation of a 3-D Seismic Volume Interpretation Workflow for Fast Track Evaluation of a Large 3-D Seismic Data Volume: Gph1/00. Curtin University of Technology.

Eaton, D., Milkereit, B., and Salisbury, M., 2003, Hardrock Seismic Exploration: Mature Technologies Adapted to New Exploration Targets.

Hossain, M., Urosevic, M., and Kepic, A., 2014. Volumetric Interpretation of 3D Seismic Data from the Hillside IOCG Deposit in South Australia. 76th EAGE Conference and Exhibition–Workshops.

Kidd, G.D., 1999, Fundamentals of 3D Seismic Volume Visualization. 1999 Offshore Technology Conference, Houston, Texas.

Ludwig, J.W., Nafe, J.E., and Drake, C.L., 1970, Seismic Refraction. in A.E. Maxwell (ed.) The Sea, 53–84.

Malehmir, A., Durrheim, R., Bellefleur, G., Urosevic, M., Juhlin, C., White, D.J., Milkereit, B., and Campbell, G., 2012, Seismic Methods in Mineral Exploration and Mine Planning: A General Overview of Past and Present Case Histories and a Look into the Future: Geophysics, 77, WC173–WC90.

Malehmir, A., Tryggvason, A., Juhlin, C., Rodriguez–Tablante, J., and Weihed, P., 2006, Seismic Imaging and Potential Field Modeling to Delineate Structures Hosting Vhms Deposits in the Skellefte Ore District, Northern Sweden: Tectonophysics, 426, 319–34.

Marjoribanks, R., 2013, Structural Interpretation of the Hillside Copper–Gold–Iron Oxide Deposit. Rex Minerals Ltd, 26.

Nafe, J.E. and Drake, C.L., 1957, Variation with Depth in Shallow and Deep Water Marine Sediments of Porosity, and the Velocities of Compressional and Shear Waves: Geophysics, 186, 523–52.

Noponen, I., Heikkinen, P., and Mehrotra, S., 1979, Applicability of Seismic Reflection Sounding in Regions of Precambrian Geology: Geoexploration, 17, 1–9.

Reed, K., 1993, Seismic Reflection Surveying for Mining Exploration Applications, a Review of Practice Past and Current with an Outlook for the Future. Unpublished report, Mineral Industry Technology Council of Canada, 219.

Salisbury, M. and Snyder, D., 2007, Application of Seismic Methods to Mineral Exploration. in W.D. Goodfellow (ed.) Mineral Deposits of Canada: A Synthesis of Major Deposit–Types, District Metallogeny, the Evolution of Geological Provinces, and Exploration Methods, Geological Association of Canada, Mineral Deposits Division, Special Publication No. 5, 971–82.

Salisbury, M.H., Milkereit, B., and Bleeker, W., 1996, Seismic Imaging of Massive Sulfide Deposits: Part I Rock Properties: Economic Geology, 91, 821–28.

Schlumberger, 2013, Schlumberger Petrel 2013 User Manual. Copyright © 2013 Schlumberger. All rights reserved.

Taner, M.T., 2001, Seismic Attributes: CSEG Recorder, 26, 48–56.

Urosevic, M., Kepic, A., Stolz, E., and Juhlin, C., 2007. Seismic Exploration of Ore Deposits in Western Australia. Proceedings of Exploration 07: Fifth Decennial International Conference on Mineral Exploration, 525–34.

Urosevic, M., Stoltz, E., and Massey, S., 2005, Seismic Exploration for Gold in a Hard Rock Environment—Yilgarn Craton, Western Australia. 67th Annual International Conference and Exhibition, EAGE, Extended Abstracts G009.

Wolfe, R.H., Jr. and Liu, C.N., 1988, Interactive Visualization of 3D Seismic Data: A Volumetric Method: IEEE Computer Graphics and Applications, 8, 24–30.

Wyss, T., Baumann, M., and Klingelé, E., 1993, Estimation of Rheological Parameters by Combined Satellite–Gravity Gradiometric and Seismic Data. Swiss Federal Institute of Technology, Institute of Geodesy and Photogrammetry.

Yilmaz, O., 1987, Seismic Data Processing / Ozdogan Yilmaz. Tulsa, OK: Society of Exploration Geophysicists.